

**FEDSM2018-83021**

## **AERODYNAMIC DRAG MEASUREMENT IN A HIGH-ENTHALPY SHOCK TUNNEL**

**Yunpeng Wang<sup>1,2,\*</sup>, Zonglin Jiang<sup>1,2</sup>, Honghui Teng<sup>3</sup>**

<sup>1</sup>State Key Laboratory of High Temperature Gas Dynamics  
Institute of Mechanics, Chinese Academy of Sciences  
Beijing 100190, China

<sup>2</sup>School of Engineering Sciences  
University of Chinese Academy of Sciences  
Beijing 100049, China

<sup>3</sup>School of Aerospace Engineering  
Beijing Institute of Technology  
Beijing 100081, China

### **INTRODUCTION**

Shock tunnels create very high temperature and pressure in the nozzle plenum and flight velocities up to Mach 20 can be simulated for aerodynamic testing of chemically reacting flows. However, this application is limited due to milliseconds of its test duration (generally 500  $\mu$ s–20 ms). For the force test in the conventional hypersonic shock tunnel, because of the instantaneous flowfield and the short test time [1–4], the mechanical vibration of the model-balance-support (MBS) system occurs and cannot be damped during a shock tunnel run. The inertial forces lead to low frequency vibrations of the model and its motion cannot be addressed through digital filtering. This implies restriction on the model's size and mass as its natural frequencies are inversely proportional the length scale of the model. As to the MBS system, sometimes, the lowest natural frequency of 1 kHz is required for the test time of typically 5 ms in order to get better measurement results [2]. The higher the natural frequencies, the better the justification for the neglected acceleration compensation. However, that is very harsh conditions to design a high-stiffness MBS structure, particularly a drag balance. Therefore, it is very hard to carried out the aerodynamic force test using traditional wind tunnel balances in the shock tunnel, though its test flow state with the high-enthalpy is closer to the real flight

condition.

Based on above issues, many balance researchers proposed several special balances to measure aerodynamic forces in the impulse facilities with high-enthalpy, that is, accelerometer balance [5–7], stress-wave force balance [8–10], free-flight measurement technique [11–16], and compensated balance [17]. Owing to the very short test time, however, the mature technology was undeveloped for the force measurements in the shock tunnel with short test duration. Based on the strain-gauge sensor's higher accuracy and sensitivity, Wang et al. [18, 19] designed a very high-stiffness pulse-type balance using the strain-gauge sensor and successfully carried out a series of force tests in a large-scale shock tunnel, which has long test duration of more than 100 ms.

In this study, a pulse-type strain-gauge balance (PSGB) was used for measuring the drag of a cone in a short-duration high-enthalpy impulse facility, JF10. The test duration is approximately 3–7 ms. Force tests were conducted for a large-scale cone with a length of 375 mm in the JF10 shock tunnel. The finite element method (FEM) was employed for the analysis of the vibrational characteristics of the MBS structure to ensure a sufficient number of cycles, particularly for the axial element structure, during 4 ms test duration (in the present flow conditions). The PSGB used in the test shows good performance, wherein the

---

\*Email: wangyunpeng@imech.ac.cn

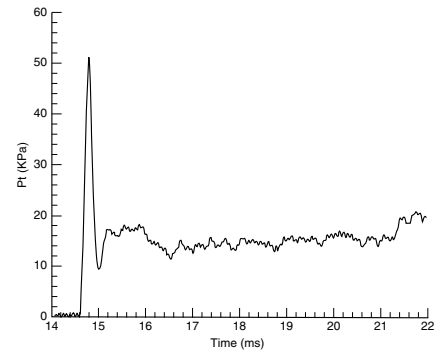
frequency of the MBS system increases because of its stiff construction. The test results were analyzed to see the effect of high-temperature gas by comparing with the data obtained in nearly ten wind tunnels.

## JF10 HIGH-ENTHALPY SHOCK TUNNEL

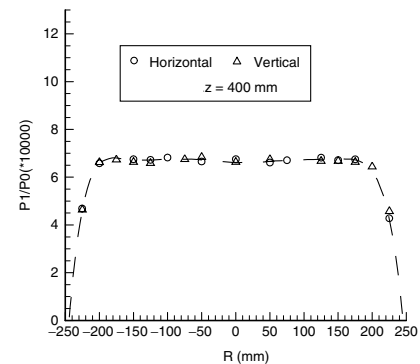
Shock tunnel is a kind of impulse ground facility, which uses a moving shock to generate high temperature and pressure test gases. The stronger the moving shock, the higher the test-gas enthalpy. Therefore, the benefits to shock tunnel are that flight velocities up to Mach 25 can be simulated. In order to develop hypersonic vehicles, it is important to develop hypervelocity test facilities for ground experimental researches. After more than 60 years development, high-enthalpy facilities suitable for studying aero-thermochemistry are still based on shock tunnels. Three kinds of high-enthalpy tunnels have been developed over the world for several decades. The first one is the heated-light-gas driven shock tunnels [20], the second one is the free-piston driven high-enthalpy shock tunnels [21–24], and another one is the detonation-driven high-enthalpy shock tunnels [25,26]. These hypersonic test facilities have been built over the world and valuable experimental data have been provided with the facilities for hypersonic study for years. JF10 in Institute of Mechanics is the first high-enthalpy shock tunnel with hydrogen and oxygen detonation-driven mode. The JF10 shock tunnel consists of three main parts. The first part is a driver being about 6.225 m in length and 150 mm in diameter, the second one is a driven section being 12.5 m in length and 100 mm in diameter, and the last is a conical nozzle having a 500 mm diameter exit. This facility can simulate some complicated physical and chemical phenomena in the hypersonic flight at high altitude, which features high-enthalpy test flow, the total enthalpy range of 15–25 MJ/kg, the total temperature of 7800–9500 K, the total pressure of 20–80 MPa, the effective test time of 3 ms to 7 ms. Figure 1 shows the Pitot pressure history and its distributions at the nozzle exit positions. It is observable that hypersonic flows in the nozzle central area appear quite uniform if evaluated from a view point of Pitot pressure distribution. This uniform flow area is found to be approximate 700 mm in length and 400 mm in diameter [27].

## MBS DESIGN AND EXPERIMENTAL DESCRIPTION

To compare with the piezoelectric sensor, the stain-gauge has enough frequency response, higher accuracy and sensitivity. We tried to use the strain-gauge transducer for measuring the aerodynamic loads in the impulse ground facility with only a few milliseconds test time. Our previous experimental and computational results, in the long-test duration shock tunnel JF12 (more than 100 ms test duration) [18, 19], show that the PSGB, with the optimized structures, can be used in the shock tunnel. There-



(a) Pitot pressure history measured at the nozzle exit



(b) Pitot pressure distributions in two directions

**FIGURE 1.** Pitot pressure measurements in JF10 nozzle flow (position  $Z = 400$  mm is a distance from the cross-section of nozzle exit)

fore, a PSGB JF12-ISG3-D053-S01 (S01 for short in this paper), which used in JF12, was employed in the present tests in short-duration shock tunnel. The balance S01 was optimized in the aspect of the measuring element of the axial load and its performance is excellent for the force measurement during 100 ms test time. From the prior FEM simulated results, the S01 has very high frequency at the axial force element (more than 2000 Hz modal frequency). The technical data of balance S01 is shown in Table 1.

**TABLE 1.** S01's technical data (mm)

Serial No.	Type	components	Diameter	Length
S01	Sting	Three	53	202.5

Figure 2 shows the details of the S01's measuring element. S01 is a three-component (i.e. axial force, normal force, and pitching moment) sting balance and uses only one rectangular-

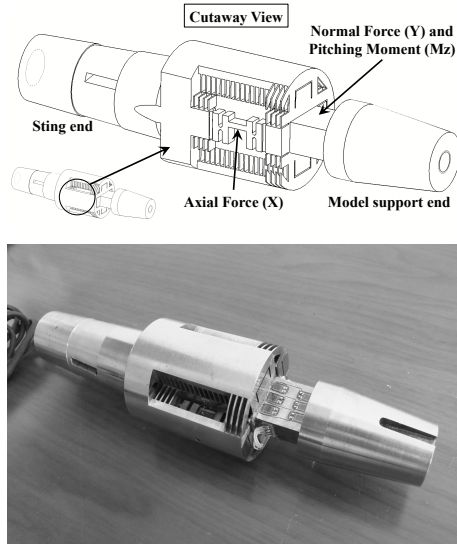


**FIGURE 2.** The S01's details of the measuring element (II-beam for the axial force element) and its photo (lower)

beam for measuring the components of normal force and pitching moment. This simple structure can increase the balance stiffness and simplify the vibration mode. The capacity of the axial force, normal force, and the pitching moment of the S01 are 1000N, 2000N, and 100 Nm, respectively.

In the JF10, the vibration is caused by the starting up of the shock tunnel and the flow establishing process. This process is very complex and usually it takes almost 1 ms. But in the following 3–7 ms, the flow will become pseudo steady. Therefore, the next tough work is to design the high-stiffness sting to support the balance and test model. In the design of the force measurement system, that is the MBS structure, we proposed a design criterion,

$$f_i = \frac{2}{t^*} \quad (1)$$

where  $f_i$  and  $t^*$  are the modal frequency of MBS in the  $i$  component (e.g. axial load) and the test duration of the impulse facility, respectively. Therefore, in the case of JF10 with the effective test time of 4 ms, the vibrational frequency of MBS in the axial component should be more than 500 Hz, so that we can find at least 2 circles in the balance output signal.

To carry out the force measurement in the impulse facility, the weight of the test model is a very important factor to determine whether the good results can be obtained. The present cone model with the  $10^\circ$  semivertex angle was made of the aluminum alloy. Its full length is 375 mm and with a maximum wall thickness of 1 mm. Therefore, its total mass is only 550 g. In addition, in order to improve the overall stiffness of MBS system, the sting

diameter is 60 mm and the cone was supported by the tail sting mounted on the support mechanism in the test section.

Prior to the shock tunnel run, the three-dimensional design of the MBS system is modeled. A series of computations, including the static structure, dynamics, and modal analysis, is conducted by using the finite element analysis. The numerical results can be used to estimate the experimental results, such as the MBS's vibrational frequency and cycle number, within the short test time. Figure 3 shows the three-dimensional modeling

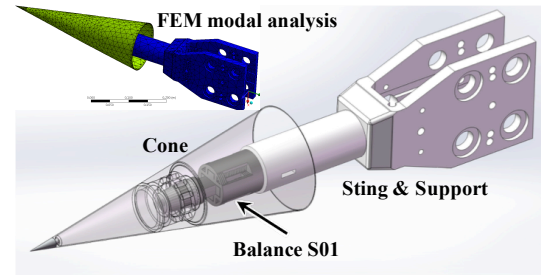


**FIGURE 3.** Diagram of the MBS system

of the MBS system. Fortunately, the frequency  $f_i$  in the present study reaches more than 1016 Hz in the axial direction. It means that at least 4 circles should be found in the balance signal within the short test time of  $t^* = 4$  ms.

## DRAG TEST AND DISSCUSION

The cone model has a large number of the test data and theoretical analysis results, so it is often used as a standard model for the flowfield calibration of new or modified wind tunnel. In the drag tests, the average stagnation pressure is 13.6 MPa and the average stagnation temperature is 7561 K. These conditions resulted in an average free-stream Mach number of 11. The drag measurements for the cone were conducted at nominal angles of attack  $0^\circ$  with  $0^\circ$  sideslip angle. Figure 4 is a photograph of the 375 mm cone model mounted in the test section.

Before the drag tests in the JF10 high-enthalpy shock tunnel, we carried out the hammer test to check the modal frequency. The force hammer with piezoelectric sensor was employed and the test is focus on the axial structure (i.e. along the drag direction). In the test, the acceleration sensor is arranged in the axial direction. The vibrational frequency is 1091Hz from the resulting of hammer test, which is consistent with the previous analysis frequency by the FEM simulation.

Figure 5 shows the balance voltage signal. As can be seen from the figure, there are four complete circles within the effective test time of 4 ms. From the test findings, the frequencies of

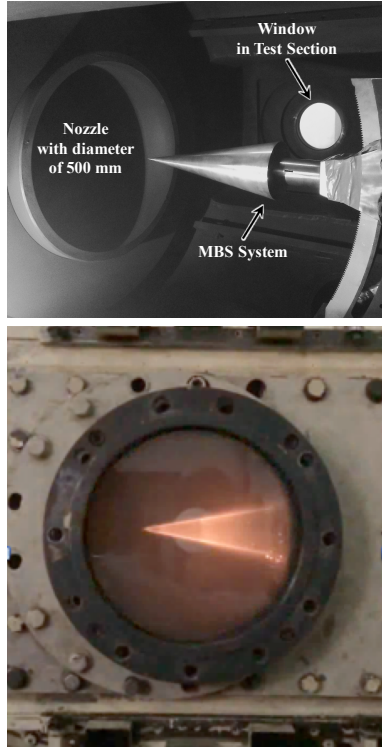


**FIGURE 4.** Photographs of MBS system in JF10's test section and the test flow over the cone during a shock tunnel run

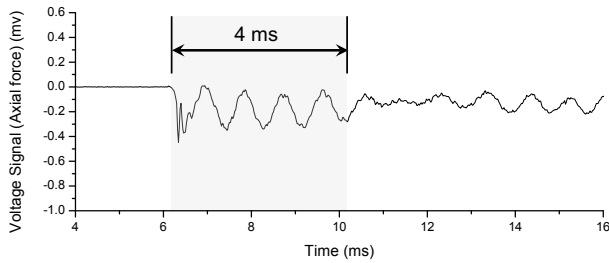


**FIGURE 5.** Voltage Signal of Balance S01

the balance signal were found using the Fast Fourier Transformation analysis and an averaged value is 1108 Hz. Obviously, this result is consistent with the results of FEM analysis (1016 Hz) and the hammer test (1091 Hz).

Furthermore, good repeatability was observed during the shock tunnel testing, where the standard deviation  $\sigma_{C_D}$  of the drag coefficient is 0.005, where the precision is less than 5%. Here, Equation 2 is used to calculate the standard deviation  $\sigma_{C_D}$ .

$$\sigma_R = \sqrt{\sum_{i=1}^n \frac{(R_i - \bar{R})^2}{n-1}} \quad (2)$$

where  $\bar{R}$  is the averaged value of some aerodynamic coefficient of  $n$  tests; in this study,  $n = 6$ . Therefore, the MBS system also shows good performance in terms of test precision.

The drag coefficient, symbolized  $C_D$ , is calculated by the following equation:

$$C_D = \frac{D}{qS} \quad (3)$$

where  $D$  is the drag (axial force);  $q$  and  $S$  represent the dynamic pressure and the reference area of the model, respectively. Fig-

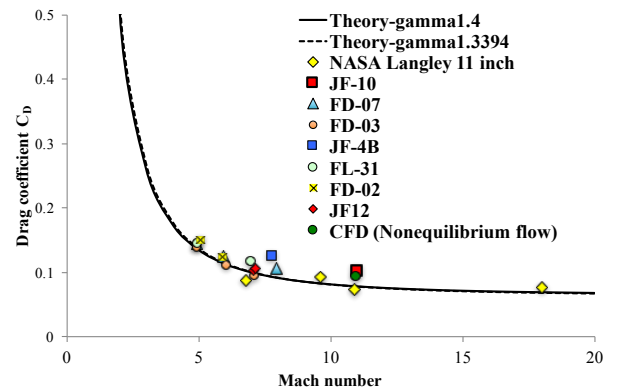


**FIGURE 6.** Comparison of the drag test results (the axial force at the  $0^\circ$  angle of attack)

ure 6 shows the present drag result compares with some data from the conventional hypersonic wind tunnels, impulse facilities, the theoretical analyses, and computational fluid dynamics (CFD) simulation. According to the above data comparisons, the present result is greater than the theoretical results. The theoretical analyses show a little effect on the ratio of specific heats  $\gamma$ , where the drag in the case of  $\gamma=1.3394$  appears to be little difference to compare with the  $\gamma=1.4$  case. In this study, the CFD simulation was carried out and the effect of the non-equilibrium flow was considered in the calculation. Compared with the CFD and theoretical results, the present drag coefficient increased by 9.476% and 30.67%, respectively.

Of course, the test results inhere some uncertainties, which are due to the systematic and random errors to determine the free stream properties, to perform the force measurements, to calibrate the balance, etc. In this paper, a preliminary analysis of the uncertainty of test results also was performed. Each kind of the error limit is combined with each kind of error limits of measured variables and constants principally because they are independent parameters. In this study, the drag coefficient is a function of the measured values of dynamic pressure and balance axial force.

In this study, a ball free-flight method is employed to directly measure the dynamic pressure by the image-processing technique, where the ball's movements (i.e. free-flight) in the flow-field are recorded by synchronized high-speed photography. [28] Dynamic pressure  $q$  measured by this method can successfully avoid the introduction of the parameter errors in the hypersonic flowfield, such as some errors confirmed by measuring the total pressure, total temperature, delta Mach number, test section wall pressure, and reference pressure. In this study, the dynamic pressure uncertainty is  $\pm 0.533$  kPa, which is approximately 5% of the averaged  $q$ . Therefore, the uncertainty assessment of testing drag becomes simple and more accurate.

The relative uncertainty in  $C_D$ , denoted  $U_{C_D}$ , is written as

$$U_{C_D} = \pm \sqrt{P_{C_D}^2 + B_{C_D}^2} \quad (4)$$

where  $P_{C_D}$  and  $B_{C_D}$  are the precision limit and bias limit of  $C_D$ , respectively. [29–31] The present results were analyzed using the confidence level of 95%. By the post-processing, a conservative assessment result is  $U_{C_D} \leq \pm 15\% C_D$ , which demonstrates the reliability of the drag measurement in the JF10 high-enthalpy hypersonic shock tunnel.

It is well known that the drag results from forces due to pressure distributions over the body surface and forces due to skin friction, which is a result of viscosity. On one hand, the pressure distributions are always somewhat insensitive to the high-temperature effects, especially for the inviscid high-temperature equilibrium flow. [32] However, the flight experience with shuttle (a blunt-body) has indicated a much higher pitching moment at hypersonic speeds than predicted. [33] In their research, due to the chemically reacting flow, the pressures are slightly higher on the forward part of the shuttle, and slightly lower on the rearward part. This results in a more positive pitching moment.

On the other hand, as is well known, the kinetic energy of a high-speed, hypersonic flow is dissipated by the influence of friction within a boundary layer. The extreme viscous dissipation that occurs within hypersonic boundary layer can create high temperatures, which can excite vibrational energy internally within molecules, and cause the dissociation and even ionization within the test gas if the temperature increased continuously. [32] Based on the CFD simulation, the static temperature of uniform flow is 400 K and the temperature in the thin hypersonic boundary layer is close to 3000 K in the JF10. As discussed previously, therefore, the vibrational energy is excited and  $O_2$  is dissociated within a chemically reacting boundary layer. The figure 4 (the right figure) also shows the high-temperature test gas over the cone and the bright light is generated on the cone's surface because of the high-enthalpy condition. Because  $O_2$  begins to dissociate above 2000 K, and is virtually completely dissociated above 4000 K. [32] In the boundary layer, the velocity gradient is getting smaller with getting thicker the boundary layer and the

shear force becomes smaller with decreasing velocity gradient. However, the temperature on the cone surface is not so high due to the cold-wall condition that the phenomenon and results become more complicated in the boundary layer. At the same time, due to the high-temperature in the hypersonic boundary layer, the viscosity increases and then the shear force (skin friction) on the model surface becomes big, which results a bigger drag.

Therefore, our preliminary point of view is that the aerodynamic drag of the cone obtained in the JF10 tests are influenced by the following aspects, i.e., (1) change of pressure distributions due to the variety of gas species, e.g. the dissociation of  $O_2$ , in the viscous high-temperature non-equilibrium flow; (2) high ratio of wall-temperature (the present model is cold-wall condition), which leads to the variety of the viscosity and the velocity gradient in the high-temperature in the boundary layer. In fact, it is unclear that the detailed mechanism of effects of the real gas thermodynamics on the aerodynamic drag. However, the current PSGB can accomplish multiple cycles of the balance signal and measure more accurate results for further understanding the complex phenomenon in the high-enthalpy flow. The test result highlights this effects of the high-enthalpy flow on the aerodynamic drag. It indicates that the real gas effects should not be ignored when the total enthalpy (or the total temperature) are high in the hypersonic flow.

In addition, the present force measurement is limited to the axial force. In the next work, the capability of the PSGB will be extended the single component to multi-component based on the present excellent performance on the drag measurement.

## SUMMARY

A strain-gauge balance was used for measuring the aerodynamic drag in a high-enthalpy hypersonic shock tunnel with approximately 4 ms test time. The strain-gauge balances are in widespread used for the force measurement in conventional wind tunnel as a mature technology but seldom works in the shock tunnel or other impulse facilities. Because the drag balance is very difficult to design and use in a short-duration ground facility due to the low frequency vibrations of the MBS by the inertial force. In the present study, a high-stiffness PSGB used in the test shows good performance, wherein the frequency of the MBS system increases because of its stiff construction. Force tests were conducted for a cone with the  $10^\circ$  semivertex angle and a length of 375 mm. The FEM simulation and the hammer test were employed for the analysis of the vibrational characteristics of the MBS system to examine a sufficient number of cycles (the axial vibration frequency) during short test duration for the axial force signal. A design criterion is proposed for the balance's structure with higher frequency to ensure at least 2 circles in the balance signal during the effective test time. The structural performance of the present PSGB is in full compliance with the requirements of drag measurement during 4 ms. Therefore, the PSGB with

optimized structure can be used for the force test in the short test duration hypersonic shock tunnel. The test results were analyzed to see the effect of high-temperature gas by comparing with the data obtained in nearly ten wind tunnels. Its standard deviation of the drag coefficient is small and the precision is less than 5%. Compared with the data obtained by the CFD and the theoretical analyses, the present drag coefficient increased by 9.476% and 30.67%, respectively. However, the detailed mechanism of the effects is still unclear, it is necessary to further study deeply. Additionally, in the future work, the capability of the current PSGB will be extended to three and six components.

## ACKNOWLEDGMENT

This work is supported by the National Natural Science Foundation of China (Grant No.11672357). The force tests were conducted in collaboration with Professor W. Zhao, Associate Professor Q. Wang, Associate Professor Y.Y. Sun, and Dr. J.W. Li. We are grateful to all their cooperation. In addition, we thank Associate Professor J. P. Li for enlightening discussions.

## REFERENCES

- [1] Arrington, P., Joiner, R., and Henderson, A., 1954. "Longitudinal characteristics of several configurations at hypersonic mach numbers in conical and contoured nozzles". *NASA TN D-2489*.
- [2] Bernstein, L., 1975. "Force measurement in short-duration hypersonic facilities". *AGARDograph No. 214*.
- [3] Naumann, K., Ende, H., Mathieu, G., and George, A., 1993. "Millisecond aerodynamic force measurement with side-jet model in the isl shock tunnel". *AIAA Journal*, **31**, pp. 1068–1074.
- [4] Naumann, K., and Ende, H., 1990. "A novel technique for aerodynamic force measurements in shock tubes". *AIP Conference Proceedings*, **208**, pp. 653–658.
- [5] Joarder, R., and Jagadeesh, G., 2003. "A new free floating accelerometer balance system for force measurements in shock tunnels". *Shock Waves*, **13**, pp. 409–412.
- [6] Saravanan, S., Jagadeesh, G., and Reddy, K., 2009. "Aerodynamic force measurement using 3-component accelerometer force balance system in a hypersonic shock tunnel". *Shock Waves*, **18**, pp. 425–435.
- [7] Sahoo, N., Mahapatra, D., Jagadeesh, G., Gopalakrishnan, S., and Reddy, K., 2003. "An accelerometer balance system for measurement of aerodynamic force coefficients over blunt bodies in a hypersonic shock tunnel". *Meas. Sci. Technol.*, **14**, pp. 260–272.
- [8] Robinson, M., Schramm, J., and Hannemann, K., 2011. "Design and implementation of an internal stress wave force balance in a shock tunnel". *CEAS Space Journal*, **1**, pp. 45–57.
- [9] Sanderson, S., Simmons, J., and Tuttle, S., 1991. "A drag measurement technique for free-piston shock tunnels". *AIAA Paper 91-0540*.
- [10] Mee, D., Daniel, W., and Simmons, J., 1996. "Three-component force balance for flows of millisecond duration". *AIAA Journal*, **34**(3), pp. 590–595.
- [11] Seiler, F., Mathieu, G., George, A., Srulijes, J., and Havermann, M., 2005. "Development of a free flight force measuring technique (ffm) at the isl shock tube laboratory". In *25th International Symposium on Shock Wave*.
- [12] Wey, P., Bastide, M., Martinez, B., Srulijes, J., and Gnemmi, P., 2012. "Determination of aerodynamic coefficients from shock tunnel free-flight trajectories". In *Proceedings of the 28th Aerodynamic Measurement Technology, Ground Testing and Flight Testing Conference*.
- [13] Martinez, B., Bastide, M., and Wey, P., 2014. "Free-flight measurement technique in shock tunnel". In *Proceedings of the 30th Aerodynamic Measurement Technology and Ground Testing Conference*.
- [14] Tanno, H., Komuro, T., Sato, K., Fujita, K., and Laurence, S., 2014. "Free-flight measurement technique in the free-piston shock tunnel hiest". *Review of Scientific Instrumentation*, **85**(045112).
- [15] Tanno, H., Komuro, T., Sato, K., Itoh, K., and Yamada, T., 2013. "Free-flight tests of reentry capsule models in free-piston shock tunnel". *AIAA Paper 2013-2979*.
- [16] Laurence, S., and Karl, S., 2010. "An improved visualization-based force-measurement technique for short-duration hypersonic facilities". *Experiments in Fluids*, **48**, pp. 949–965.
- [17] Marineau, E., MacLean, M., Mundy, E., and Holden, M., 2012. "Force measurements in hypervelocity flows with an acceleration compensated strain gage balance". *Journal of Spacecraft and Rockets*, **49**(3), pp. 474–482.
- [18] Wang, Y., Liu, Y., Luo, C., and Jiang, Z., 2016. "Force measurement using strain-gauge balance in a shock tunnel with long test duration". *Review of Scientific Instruments*, **87**(055108).
- [19] Wang, Y., Liu, Y., and Jiang, Z., 2016. "Design of a pulse-type strain gauge balance for a long-test-duration hypersonic shock tunnel". *Shock Waves*, **26**(6), pp. 835–844.
- [20] Holden, M., 1993. "Recent advances in hypersonic test facilities and experimental research". *AIAA 93-5005*.
- [21] Stalker, R., 1987. "Shock tunnel for real gas hypersonics". *AGARD Conference Proceedings*, **428**.
- [22] Burstchell, Y., Brun, R., and Zeitoun, D., 1991. "Two dimensional numerical simulation of the marseille university free-piston shock tunnel tcm2". *Proceedings of the 18th International Symposium on Shock Wave*, **1**, pp. 583–590.
- [23] Hornung, H., 1992. "Performance data of the new free-piston shock tunnel at galcit". *AIAA 92-3943*.
- [24] Itoh, K., Ueda, S., Komuro, T., Sato, K., Tanno, H., and

- Takahashi, M., 1999. "Hypervelocity aerothermodynamic and propulsion research using a high enthalpy shock tunnel hiest". *AIAA 99-4960*.
- [25] Yu, H., Esser, B., Lenartz, M., and Gronig, H., 1992. "Gaseous detonation driver for a shock tunnel". *Shock Waves*, **2**, pp. 245–254.
- [26] Zhao, W., Jiang, Z., Saito, T., Lin, J., Yu, H., and Takayama, K., 2005. "Performance of a detonation driven shock tunnel". *Shock Waves*, **14**(1–2), pp. 53–59.
- [27] Jiang, Z., Lin, J., and Zhao, W., 2012. "Performance tests of jf-10 high-enthalpy shock tunnel with a fdc driver". *International Journal of Hypersonics*, **2**(1), pp. 29–36.
- [28] Ma, J., Tang, Z., and Zhang, X., 1983. "Free flight method in hypersonic impulse type tunnels for static and dynamic stability study". *Acta Aerodynamica Sinica (in Chinese)*(4), pp. 82–90.
- [29] 15, F. D. P. W. G., 1994. "Quality assessment for wind tunnel testing". *AGARD-AR-304*.
- [30] Standard, A., 1999. *Assessment of experimental uncertainty with application to wind tunnel testing (AIAA S-071A-1999)*. American Institute of Aeronautics and Astronautics, VA, USA.
- [31] Guide, A., 2003. *Assessing Experimental Uncertainty – Supplement to AIAA S-071A-1999 (AIAA G-045-2003)*. American Institute of Aeronautics and Astronautics, VA, USA.
- [32] Anderson, J. D., 2006. *Hypersonic and High-Temperature Gas Dynamics, Second Edition*. American Institute of Aeronautics and Astronautics.
- [33] Maus, J. R., Griffith, B. J., Szema, K. Y., and Best, J. T., 1984. "Hypersonic mach number and real gas effects on space shuttle orbiter aerodynamics". *Journal of Spacecraft and Rockets*, **21**(2), pp. 136–141.